Biosensors and Bioelectronics 38 (2012) 402–406

Contents lists available at SciVerse ScienceDirect

Biosensors and Bioelectronics

journal homepage: www.elsevier.com/locate/bios

Short communication

Controllable anchoring of gold nanoparticles to polypyrrole nanofibers by hydrogen bonding and their application in nonenzymatic glucose sensors

Cuiling Li [a], Yi Su [a], Xiangyu Lv [a], Hailong Xia [b], Hongjun Shi [a], Xiangguang Yang [a], Jinqiang Zhang [c], Yujiang Wang [a,*]

[a] Changchun Institute of Applied Chemistry, Graduate School of Chinese Academy of Sciences, 5625 Renmin Street, Changchun 130022, PR China
[b] Rush University Medical Center, 1653 West Congress Parkway, Chicargo, IL 60612, USA
[c] Key Laboratory of Middle Atmosphere and Global Environment Observation, Institute of Atmospheric Physics, Chinese Academy of Sciences, Beijing 100029, PR China

ARTICLE INFO

Article history:
Received 3 February 2012
Received in revised form
12 April 2012
Accepted 13 April 2012
Available online 11 May 2012

Keywords:
Polypyrrole
Au/PPyNFs
Hydrogen bonding
Glucose sensors
Biosensors

ABSTRACT

An enzymeless glucose biosensor based on polypyrrole nanofibers-supporting Au nanoparticles (Au/PPyNFs) was investigated in this study. The Au/PPyNFs heterogeneous composite materials were synthesized in-situ via hydrogen bonding interactions for the assembly of polyethyleneimine (PEI) on the surface of polypyrrole nanofibers (PPyNFs). By changing the molar ratio of PPy to $HAuCl_4$, Au/PPyNFs with different Au loadings were obtained. The morphology and composition of Au/PPyNFs were characterized using SEM, TEM, FTIR, XRD and XPS, respectively. The hybrids exhibited a high electrocatalytic activity toward glucose oxidation, which is prerequisite for the catalysts to be applied in amperometric glucose sensors. By using the nonenzymatic glucose sensor based on Au/PPyNFs, 0.2–13 mM glucose can be detected with a sensitivity of 1.003 $\mu A\,cm^{-2}\,mM^{-1}$ and a good linearity ($R^2=0.9993$) between current density and glucose concentration. The proposed glucose sensor provides a promising strategy to construct fast, sensitive, and anti-interfering amperometric sensors for early diagnosis and prevention of diabetes.

1. Introduction

Diabetes mellitus is a worldwide public health problem. This metabolic disorder results from insulin deficiency and is reflected by blood glucose concentrations higher or lower than the normal range 80–120 mg dL^{-1} (4.4–6.6 mM) (Wang, 2008). The diagnosis and management of diabetes thus requires glucose sensors to monitor blood glucose levels. Since Clark and Lyons reported the first enzyme electrode in 1962 (Clark et al., 1962), the efforts to develop and improve glucose sensors, particularly based on amperometry, have been made in the past 50 years. The widely studied amperometric glucose sensors fell into two types, the enzymatic and enzymeless sensors. Although enzymatic detection usually shows good selectivity and high sensitivity, the most common and serious problem of enzymatic glucose sensors lie in their lack of long-term stability owing to the nature of enzymes (Li et al., 2010a,b; Xia et al., 2011; Yuan et al., 2005). As a result, much effort has focused on amperometric glucose sensors to improve the stable performance of glucose sensors.

The electrochemical oxidation of glucose has been extensively studied in relation to electrochemical sensors. It has been proved that Au is an attractive metal for the oxidation of glucose and the catalytic activity of Au toward glucose oxidation could be increased by depositing Au nanoparticles (NPs) on supporting matrix (Ryu et al., 2010; Si et al., 2011; Tominaga et al., 2005; Wang et al., 2011). As one of the leading conducting polymers, polypyrrole nanofibers (PPyNFs) have attracted considerable attention to be used as supporting matrix in electrochemical sensors because of their good physical and electrical properties, excellent environment stability and biocompatibility, and ease of preparation (Liu et al., 2011; Sekine et al., 2010; Zang et al., 2008). Also, using PPyNFs as supports could avoid harsh oxidation pretreatment and get a good dispersion of metal NPs for the intrinsic existence of functional groups and long carbon chains (Bai et al., 2011; Correa-Duarte et al., 2004). Therefore, it is pertinent to deposit Au NPs on the surface of PPyNFs (Au/PPyNFs) in a facile way to improve their catalytic activity toward glucose oxidation with less Au consumption.

To prepare high-quality supported metal catalysts, one must be able to deposit dispersed metal NPs, preferably with sizes in the nanometer range, on supporting materials. Depositing Au NPs on PPy tubules have been achieved with electrodeposition and physisorption (He et al., 2005; Li and Lin, 2007; Qiu et al., 2011). However, in most cases, poor dispersion, large metal NPs and desquamation were found for these deposition methods, especially under high loading conditions. It is desirable and feasible to use the function of –NH-group in the PPyNFs to get good deposition of metal NPs. As is known, there is

* Corresponding author. Tel./fax: +86 431 85262325.
E-mail address: wangyj@ciac.jl.cn (Y. Wang).

0956-5663/$ - see front matter © 2012 Elsevier B.V. All rights reserved.
http://dx.doi.org/10.1016/j.bios.2012.04.049

hydrogen bonding in the compounds containing atoms with lone pair of electrons, such as H_2O, PPy, PEI and polyaniline, and the cooperative interactions increase apparently when involving more molecules (Drury et al., 2007; Kobko et al., 2001; Zang et al., 2008). Here, we report a unique chemical reduction route to coat PPyNFs with controllable coverage of Au NPs by means of hydrogen bonding interactions. In this approach linear PEI is used as not only a functionalizing agent for the PPyNFs but also a reducing agent for the formation of Au NPs.

After its successful synthesis, Au/PPyNFs were developed as the electrocatalysts for the oxidation of glucose in this work. An amperometric glucose sensor was then fabricated based on the Au/PPyNFs and its properties, such as sensitivity, selectivity and stability in the glucose detection were investigated here.

2. Experimental

2.1. Synthetic procedures

Scheme 1 shows the schematic procedure for the preparation of Au/PPyNFs hybrids. The produced PPyNFs (4 mg) and PEI (160 mg) were dispersed in 40 mL of deionized water under ultrasonication. Four samples were prepared according to the following procedure: 10 mL of as-prepared mixed solution was placed in a vial and heated to 80 °C under vigorous stirring. To the four respective mixed solutions, $HAuCl_4$ (4.86 mM) with initial molar ratios of 2:1, 1:1, 1:2 and 1:3 of PPy to $HAuCl_4$ was added. All the resulting solutions were kept at 80 °C for 40 min. After being washed and centrifuged with ethanol and deionized water for three times, the resulted products were dried in vacuum oven at 60 °C for 10 h. Corresponding to the different molar ratios, the obtained samples were named Au/PPyNFs-1, Au/PPyNFs-2, Au/PPyNFs-3 and Au/PPyNFs-4.

PPyNFs were synthesized using a self-assembled surfactant template method as reported in the literature with some modification (Zhang et al., 2006). The Au NPs were synthesized based on the method reported before (Li et al., 2010a,b). The details were shown in supplementary material.

2.2. Electrochemical measurements

Electrochemical experiments were performed with a CHI 660D electrochemical workstation in a conventional three-electrode cell using glassy carbon electrode (GCE, 3 mm diameter), Pt foil and Ag/AgCl (saturated KCl) as the working electrode, auxiliary electrode and reference electrode, respectively. The Au NPs, Au/PPyNFs hybrids were ultrasonically dispersed in 0.5% Nafion solution to form a homogeneous dispersion (25 mg mL^{-1}). Then, 5 μL of the dispersion was casted onto the surface of pre-treated GCE, and dried in air before the electrochemical experiments. The hydrodynamic amperometric measurements required operation of the electrode at a constant applied potential of 0.25 V vs. Ag/AgCl in 0.1 M NaOH. The cyclic voltammetry (CV) measurements were carried out both in 0.1 M NaOH and in 0.1 M phosphate buffer solution (PBS, pH 7.4) electrolyte under ambient air. All potential values were referenced to Ag/AgCl (saturated KCl) electrode.

2.3. Physical characterization

The morphology of the PPyNFs, Au and Au/PPyNFs hybrids were characterized by TEM (JEOL JEM 2010) and FESEM (S-4800, Hitachi). The X-ray diffraction (XRD) patterns for the hybrids were obtained using a Rigaku-D/MAX-PC2500 X-ray diffractometer with the CuKα (λ=1.5405 Å) radiation source operating at 40 kV and 200 mA. The composition of the prepared hybrids was evaluated by XPS measurements, and conducted with an ESCALAB MK II spectrometer (VG Co., UK) with MgKα radiation ($h\upsilon$=1253.6 eV) as the X-ray source and a pass energy of 20 eV. The pressure inside the analyzer was maintained at 6.5×10^{-7} Pa.

3. Results and discussion

3.1. Characterization of Au/PPyNFs

Hydrogen bonding, which is the driving force in the functionalization of PPyNFs could be detected by IR spectra

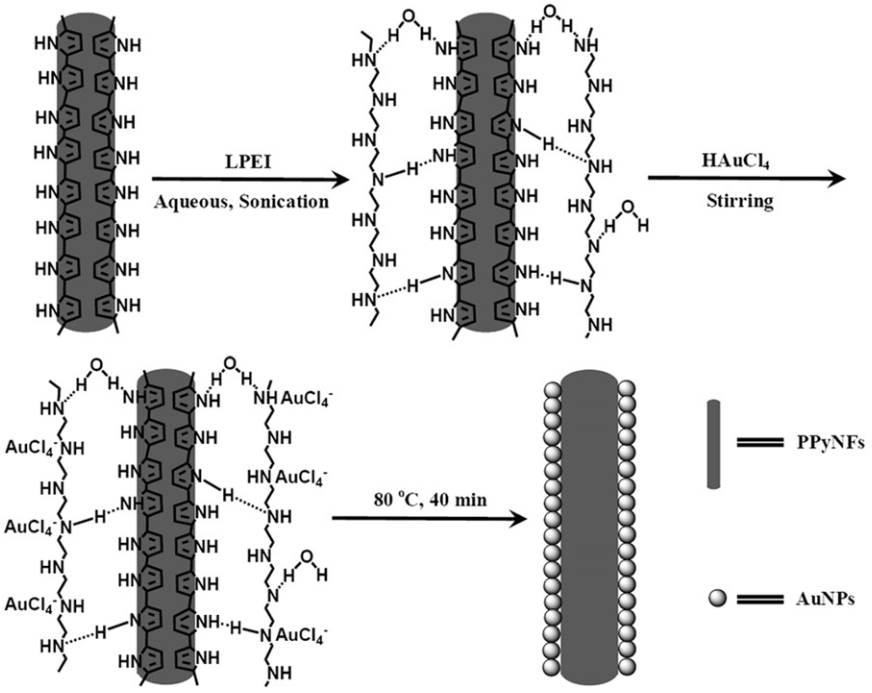

Scheme 1. Schematic diagram of the procedure for the synthesis of Au/PPyNFs hybrids.

(Hashida et al., 2002; Herlem et al., 2010). Hence, PEI, pristine PPyNFs and PEI-functionalized PPyNFs (PEI–PPy) were characterized by Fourier transform infrared spectroscopy (FTIR) (Fig. S1). Overall, the IR spectra of PEI-functionalized PPyNFs show peaks that are characteristic of the main functional groups of PEI and pristine PPyNFs. However, there are distinct differences between the IR spectrum of PEI–PPyNFs complex and that of pristine PPyNFs or PEI alone. All the differences illuminated the formation of hydrogen bonds. The band at 880 cm^{-1} assigned to the anhydrate of PEI disappeared in the PEI–PPyNFs. Correspondingly, the red shift in the N–H stretching vibration at ~3400 cm^{-1} and the emergence of band at 938 cm^{-1} confirmed the hydrate of PEI and PPyNFs (Hashida et al., 2002; Herlem et al., 2010; Vallejos et al., 2010; York et al., 2003). Furthermore, the broad absorption band at 3500–3400 cm^{-1}, may be assigned to the stretching vibration of absorbed water, which acted as bridge between PEI and PPyNFs chains by hydrogen bond, as depicted in Scheme 1 (Angelina and Peruchena, 2011; Boesch et al., 2001; Hashida et al., 2002).

The morphology and microstructure of PPyNFs and Au/PPyNFs-3 were examined with SEM and TEM. It can be clearly seen that the PPyNFs exhibit an average diameter of about 60 nm and a length of several micrometers (Fig. 1a and b). From Fig. 1c–e, it can be seen that high-density and well-dispersed Au NPs have been deposited on the surfaces of PPyNFs without observable particle aggregation. The size distribution of Au NPs evaluated statistically from 300 Au NPs shown in Fig. 1e indicated that Au NPs ranged in diameter from 3.2 to 9.0 nm with a mean diameter of 6.5 nm, as shown in Fig. 1f. This strategy provided a general route to obtain Au/PPyNFs hybrids with different Au contents. Figs. S2–S5 illuminated that the loading of Au NPs on the surface of the PPyNFs could be easily controlled by changing the molar ratio of PPy and $HAuCl_4$. At molar ratio 1:2, the loading of Au NPs was in good dispersion and high coverage.

The formation of Au/PPyNFs hybrids was further confirmed by X-ray diffraction (XRD) and X-ray photoelectron spectroscopy (XPS) (Figs. S6 and S7). The diffraction peaks at 38.4°, 44.5°, 64.8°, 77.8° and 81.7° are ascribed to (111), (200), (220), (311) and (222) planes of Au face-centered cubic (fcc) crystallographic structures (Guo et al., 2007). The average size of Au NPs calculated using the Debye–Scherrer equation is 6.5 nm, which agrees well with the TEM results. XPS plots of Au/PPyNFs powders show characteristic signals for Au, C, N and O (Fig. S7). The N1s spectrum was deconvoluted into three component peaks, with main contribution of binding energy at 399.4 eV. The peak at 399.4 eV is attributed to neutral nitrogen moieties (–NH-) in PPyNFs and PEI (Sun et al., 2011; Zinovyeva et al., 2011). A smaller peak at 397.9 eV is usually assigned to uncharged deprotonated imine (=N-) atoms. The hydrogen bonding induces the deprotonation, which involves exclusively transformation of $-N^{+}-$ to =N-groups. That is why the peak of =N- is shown in the N spectrum and also proves the existence of hydrogen bonding interaction between PEI and water. C1s signal was deconvoluted into three components in which the peak at 284.5 eV is attributed to C_α and C_β polypyrrole atoms (Hasik et al., 2003; Neoh et al., 1997). Fig. S7-d showed the Au4f deconvolution spectrum of Au/PPyNFs-3. The doublet peaks located at 84 eV ($Au4f^{7/2}$) and 87.7 eV ($Au4f^{5/2}$) are signatures for Au^0 (Neoh et al., 1997). All the XPS results confirmed the formation of Au NPs on the surface of PPyNFs.

3.2. Sensor performance

It is generally accepted that AuOH sites on the Au surfaces act as the active species for glucose oxidation and the oxidation of glucose is strongly dependent on the number of AuOH sites (Wang et al., 2011). Hence, the electrochemical activity of Au/PPyNFs-3 towards glucose oxidation was first tested in different electrolytes, as shown in Fig. 2a. It is obvious that the NaOH electrolyte results in both an increase of peak current and a negative shift of peak potential. Consequently, NaOH is a superior electrolyte for improving the electrocatalytic activity of Au/PPyNFs and 0.1 M NaOH was chosen as electrolyte in the following tests. Then, the effect of Au content towards glucose oxidation

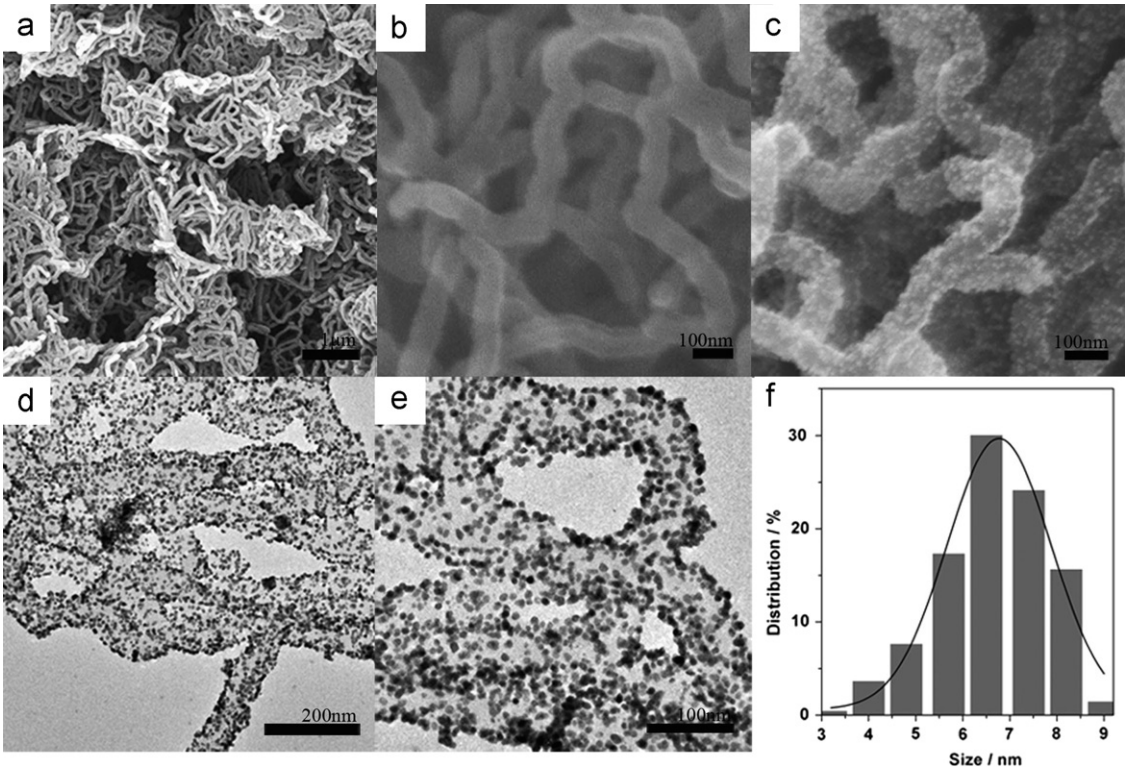

Fig. 1. (a), (b) SEM images of PPyNFs. (c) SEM and (d), (e) TEM images of Au/PPyNFs hybrids at different magnifications. (f) Size distribution of Au NPs in (e).

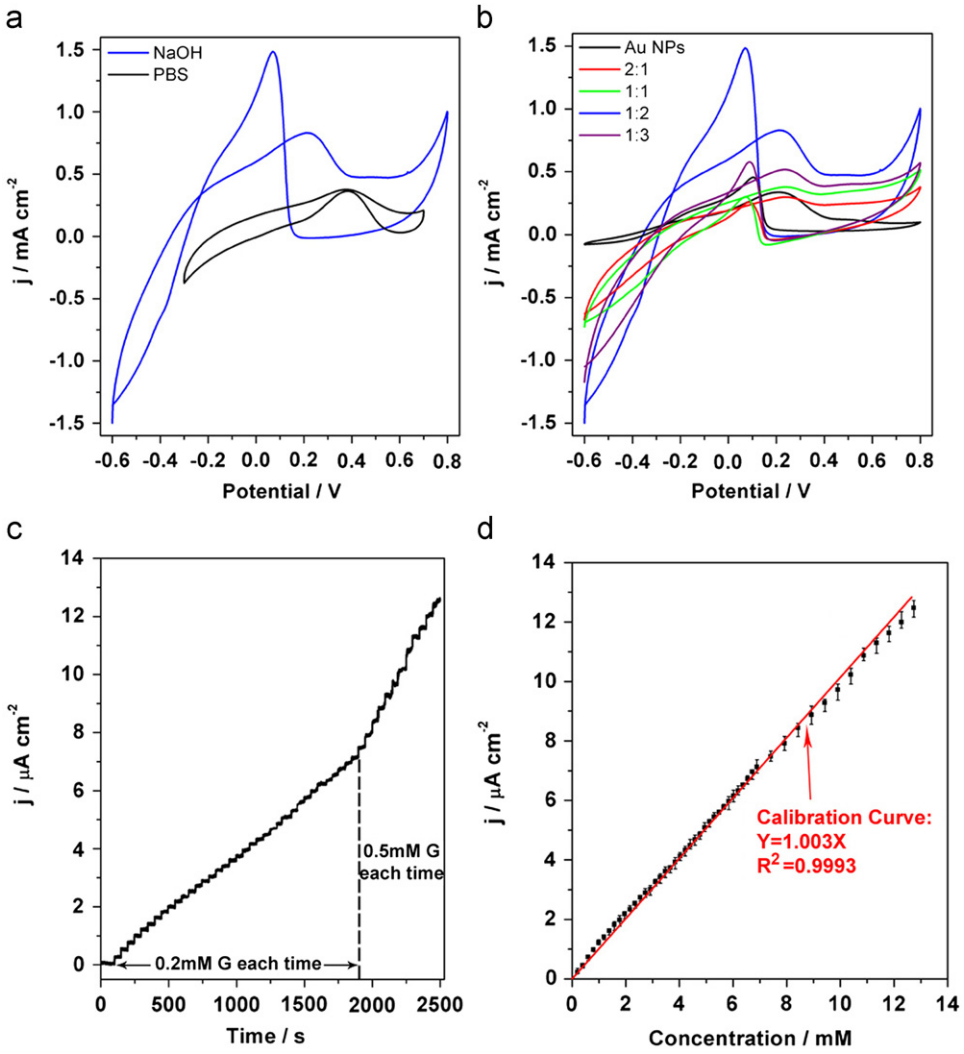

Fig. 2. (a) CVs of Au/PPyNFs-3 in 0.1 M NaOH and 0.1 M PBS (pH 7.4) containing 20 mM glucose; (b) CVs of Au NPs, Au/PPyNFs-1, Au/PPyNFs-2, Au/PPyNFs-3 and Au/PPyNFs-4 in 0.1 M NaOH containing 20 mM glucose; (c) Hydrodynamic amperometric response of the sensor based on Au/PPyNFs-3 to successive additions of glucose and (d) its corresponding calibration curve. The error bars represent the standard deviations detected for three times.

was further studied by using different catalysts and the results were shown in Fig. 2b. It can be seen that glucose shows much stronger redox peaks at the as-prepared Au/PPyNFs electrode and the catalytic activity of Au/PPyNFs varies with the loading of Au NPs. As can be seen from Fig. 2b, the Au/PPyNFs-3 showed the best catalytic activities toward glucose. This may be attributed to the well dispersion of Au NPs on PPyNFs and gaps between Au NPs, which are favorable for the mass and electron transfer (Dennany et al., 2008; Li et al., 2010a,b). Fig. 2c showed the hydrodynamic amperometric responses of the glucose sensor based on Au/PPyNFs-3 with successive increments of glucose concentration from 0.2 to 13 mM. A rapid increase in the current after each addition of glucose was noticed. From the calibration curve shown in Fig. 2d, it can be seen that the proposed sensor displays a linear response (R^2=0.9993) to glucose with a sensitivity of 1.003 μA cm^{-2} mM^{-1}. The error bars represent the standard deviations detected three times. The anti-interfering performance of the proposed glucose sensor has also been tested. It has been reported that the concentration of interfering species is about one 20th of that of glucose. Hence, the interference effect of 0.1 mM urea and 0.1 mM ascorbic acid on the amperometric response of 2 mM glucose was studied. As showing in Fig. S8, the sensor based on Au/PPyNFs-3 could be used to detect glucose in the presence of urea and ascorbic acid.

4. Conclusion

In summary, we have demonstrated a novel and simple in-situ synthetic route for the preparation and coverage control of Au/PPyNFs heterogeneous composite materials. These Au/PPyNFs hybrids have been confirmed to be very effective as electrocatalysts toward glucose oxidation. The amperometric glucose sensor based on Au/PPyNFs-3 showed a good linearity (R^2=0.9993) between current response and glucose concentration. The Au/PPyNFs hybrids with high catalytic activities are easily synthesized and can be assembled to be an amperometric nonenzymatic sensor for routine analysis of glucose in clinical diagnostics.

Acknowledgment

This work was supported by a Grant-in-Aid for Development of New Oxygen Sensors and Apparatus used for Oxygen Detection (20030309) from the Department of Science and Technology of Jilin province.

Appendix A. Supporting information

Supplementary data associated with this article can be found in the online version at http://dx.doi.org/10.1016/j.bios.2012.04.049.

References

Angelina, E.L., Peruchena, N.M., 2011. Journal of Physical Chemistry 115, 4701–4710.

Bai, Z.Y., Yang, L., Cuo, Y.M., Zhang, Z., Hu, C.G., X, P.L., 2011. Chemical Communications 47, 1752–1754.

Boesch, S.E., York, S.S., Frech, R., Wheeler, R.A., 2001. PhysChemComm 4, 1–10.

Clark, J.L.C., Lyons, C., Aead, A.N.Y., 1962. Science 102, 29–45.

Correa-Duarte, M.A., Sobal, N., Liz-Marzán, L.M., Giersig, M., 2004. Advanced Materials 16, 2179–2184.

Dennany, L., O'Reilly, E.J., Innis, P.C., Wallace, G.G., Forster, R.J., 2008. Electrochimica Acta 53, 4599–4605.

Drury, A., Chaure, S., Kröll, M., Nicolosi, V., Chaure, N., Blau, W.J., 2007. Chemistry of Materials 19, 4252–4258.

Guo, S.J., Wang, L., Wang, E.K., 2007. Chemical Communications, 3163–3165.

Hashida, T., Tashiro, K., Aoshima, S., Inaki, Y., 2002. Macromolecules 35, 4330–4336.

Hasik, M., Bernasik, A., Adamczyk, A., Malata, G., Kowalski, K., Camra, J., 2003. European Polymer Journal 39, 1669–1678.

He, Y.H., Yuan, J.Y., Shi, G.Q., 2005. Journal of Materials Chemistry 15, 859–862.

Herlem, G., Gharbi, T., Sedrine, N.B., 2010. Journal of Molecular Structure 945, 27–32.

Kobko, N., Paraskevas, L., Rio, E., Dannenberg, J.J., 2001. Journal of the American Chemical Society 123, 4348–4349.

Li, C.L., Su, Y., Lv, X.Y., Xia, H.L., Wang, Y.J., 2010a. Sensors and Actuators B 149, 427–431.

Li, C.L., Su, Y., Zhang, S.W., Lv, X.Y., Xia, H.L., Wang, Y.J., 2010b. Biosensors and Bioelectronics 26, 903–907.

Li, J., Lin, X.Q., 2007. Sensors and Actuators B 126, 527–535.

Liu, M.J., Liu, X.L., Ding, C.M., Wei, Z.X., Zhu, Y., Jiang, L., 2011. Soft Matter 7, 4163–4165.

Neoh, K.G., Young, T.T., Looi, N.T., Kang, E.T., 1997. Chemistry of Materials 9, 2906–2912.

Qiu, L.H., Liu, B.Q., Peng, Y.J., Yan, F., 2011. Chemical Communications 47, 2934–2936.

Ryu, J., Kim, K., Kim, H.-S., Hahn, H.T., Lashmore, D., 2010. Biosensors and Bioelectronics 26, 602–607.

Sekine, S., Ido, Y., Miyake, T., Nagamine, K., Nishizawa, M., 2010. Journal of the American Chemical Society 132, 13174–13175.

Si, P., Kannan, P., Guo, L.H., Son, H.S., Kim, D.-H., 2011. Biosensors and Bioelectronics 26, 3845–3851.

Sun, X.-F., Wang, S.-G., Cheng, W., Fan, M., Tian, B.-H., Gao, B.-Y., Li, X.-M., 2011. Journal of Hazardous Materials 189, 27–33.

Tominaga, M., Shimazoe, T., Nagashima, M., Taniguchi, I., 2005. Electrochemistry Communications 7, 189–193.

Vallejos, M.M., Angelina, E.L., Peruchena, N.M., 2010. Journal of Physical Chemistry A 114, 2855–2863.

Wang, J., 2008. Chemical Reviews 108, 814–825.

Wang, J.F., Gong, J.X., Xiong, Y.S., Yang, J.D., Gao, Y., Liu, Y.L., Lu, X.Q., Tang, Z.Y., 2011. Chemical Communications 47, 6894–6896.

Xia, Y., Huang, W., Zheng, J.F., Niu, Z.J., Li, Z.L., 2011. Biosensors and Bioelectronics 26, 3555–3561.

York, S.S., Boesch, S.E., Wheeler, R.A., Frech, R., 2003. Macromolecules 36, 7348–7351.

Yuan, J.H., Wang, K., Xia, X.H., 2005. Advanced Functional Materials 15, 803–809.

Zang, J.F., Li, C.M., Bao, S.-J., Cui, X.Q., Bao, Q.L., Sun, C.Q., 2008. Macromolecules 41, 7053–7057.

Zhang, X.T., Zhang, J., Song, W.H., Liu, Z.F., 2006. Journal of Physical Chemistry B 110, 1158–1165.

Zinovyeva, V.A., Vorotyntsev, M.A., Bezverkhyy, I., Chaumont, D., Hierso, J.-C., 2011. Advanced Functional Materials 21, 1064–1075.